NONLINEAR MODELING OF A MAGNETICALLY GUIDED MACHINE TOOL AXIS

Martin Ruskowski
Institut für Mechanik, Universität Hannover, Germany, mrusk@ifm.uni-hannover.de
Karl Popp
Institut für Mechanik, Universität Hannover, Germany, popp@ifm.uni-hannover.de

ABSTRACT

Contactless linear magnetic guides qualify as an alternative guiding principle for high speed cutting (HSC) machines, as they avoid frictional forces and wear. Tests on a prototype guide showed, that an adequate dynamic stiffness for a machine tool axis can be achieved with a magnetic guide. For the application to a prototype machine the concept has to be modified to fulfil the demands of machine design. This requires a new type of magnet arrangement as well as new models for the active parts. A new structure of magnetic guides is proposed basing on nonlinear models of the guiding magnets. Further, influences of eddy current effects and appropriate countermeasures will be discussed. The resulting machine axis will allow a dynamical stiffness of the guide of up to 150N/μm in the whole frequency range at a damping ratio near D=1.

INTRODUCTION

The new generation of High Speed Cutting (HSC) machine tools requires a completely new approach for design. Next to the drives and the machine structure, the guides are one of the main limiting factors for speed and acceleration of the machine. Contactless magnetic guides offer a large potential to serve as a guiding principle in high-end milling machines. They have superior properties compared to conventional linear roller bearings concerning friction effects and wear.

Figure 1 shows the design sketch for a prototype milling machine under development at Hannover University. This machine is developed in a joint interdisciplinary project and aims at an acceleration of 3g in all axes. It will be the first milling machine worldwide based on magnetic guides. The considered design incorporates a conventionally guided, directly driven, vertical cross-arrangement for the work piece. The milling spindle is fixed to a horizontal magnetically guided axis with two differential direct drives.

Although a prototype guide (cp. figure 2, left) exists at our institute for several years now [1-2], and a larger, driven axis has been build based on our design and control strategy [3], the design of a magnetic guide for implementation in a milling machine requires a completely different approach than that of the prototype guide. The

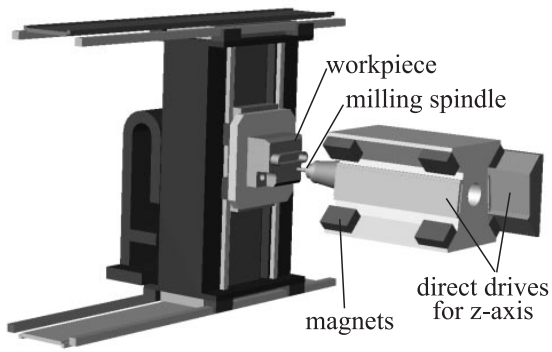

FIGURE 1: Sketch of new HSC milling machine

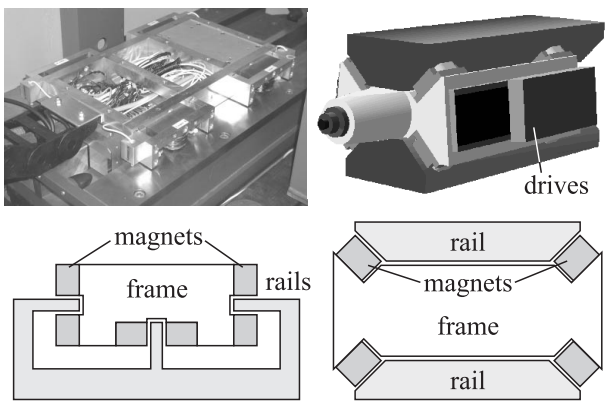

FIGURE 2: Prototype guide and model of new machine axis along with their magnet arrangements

traditional differential magnet arrangements used so far show advantages with respect to magnet force linearity but they are difficult to apply for mechanical reasons, as this incorporates weak rails and a larger number of guiding magnets.
The guides realized so far use a differential arrangement of 12 magnets at 6 load positions. Instead, a symmetrical single magnet arrangement of 8 magnets in 2 arrays (cp. figure 2, right) shows to be a better choice [4]. The main disadvantage of a single magnet arrangement is the nonlinear current-force-displacement characteristics, as no more hardware linearization is available. To compensate for this, a software linearization has been developed, which approximates the inverted magnet characteristics via simple analytical functions. Whether the rails are fixed vertically (cp. figure 1) or horizontally (cp. figure 2) is a matter of the specific design. Horizontal rails will be used for the new machine.
Due to mechanical and machining reasons, the guiding rails used so far [1-3] have been made of solid steel. This is mostly because of the differential magnet arrangement making the fastening of laminated rails difficult or impossible. Massive steel rails limit the magnet dynamics at higher frequencies due to eddy-current losses. A possible countermeasure for solid rails will be discussed later. The new magnet concept allows an easy implementation of laminated rails by applying a laminated layer on top of the trapezoidal rails.

MACHINE DESIGN

The basic design of a magnetic guide requires a mechanical arrangement guaranteeing the controllability of the levitation. Especially the rotatory movements have to be taken into account. The proposed configuration allows the control of all rigid body modes of the guide while representing a symmetrical magnet distribution. The feed direction of the guide is driven by two linear synchronous motors in double comb arrangement, so the parasitical high normal forces of the drives compensate each other.
The mass of the guide and thereby the static load due to gravity requires a constant levitating force in vertical direction. For small guides, this force can be applied to the guiding magnets themselves. For larger guides additional permanent magnets can be applied [3]. At a close look both concepts are not optimal. A better way is to use the normal forces of the drives for the static levitation by slanting the motors (cp. figure 3, patent pending).

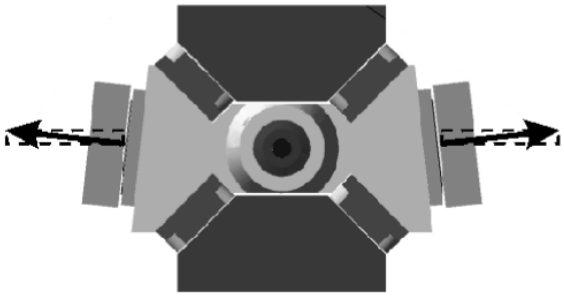

FIGURE 3: Compensation of the static load using the feed drives [5]

Another feature of the magnetic guides used in the machine design is the ability to vary the air gap. Small correction movements can be performed to compensate for position errors in the conventionally guided axes. First tests of such a hybrid drive show that the position accuracy increases especially at high frequency motions, whereas the accuracy of the conventionally guided axis is hindered by the discontinuous friction force.

MECHANICAL MODELING

As a first approach, the guide frame itself can be supposed to be a rigid body. The feed drive will at first be left out of consideration. Its implementation in the control loop can be very easily performed. Thus, the control has to be designed for 5 degrees of freedom (d.o.f.). Figure 4 shows the free body diagram the controller design is based upon.

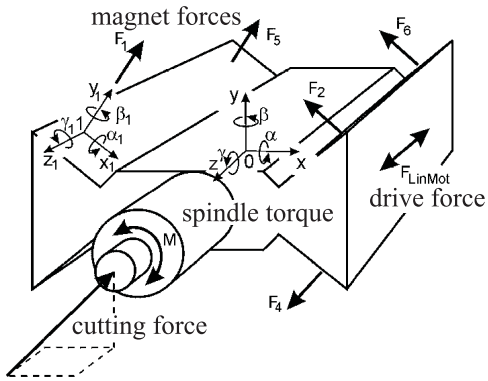

FIGURE 4: Free body diagram of the machine axis [5]

A finite element analysis of the frame shows the torsional mode to be the first flexible mode. With a natural frequency of 683Hz it is the only flexible mode having to be modeled, as all other flexible modes have natural frequencies far above 1000Hz. As the torsional motion of the frame can be measured directly by the displacement sensors next to each electromagnet, the model can be expanded to 6 degrees of freedom. An additional controller can be used to damp the torsional mode. This enables higher controller dynamics for the rigid body modes, as spill over effects destabelizing the torsional mode can be reduced [7].

CONTROL STRATEGY

The control strategy used for the machine axis has been previously published [1-2]. It can be easily adapted to the new machine structure with 8 actuating electromagnets.
The basic idea of the controller is to decouple the 5 controlled degrees of freedom via an invese model of the (constant) couplings in the plant. This is performed via

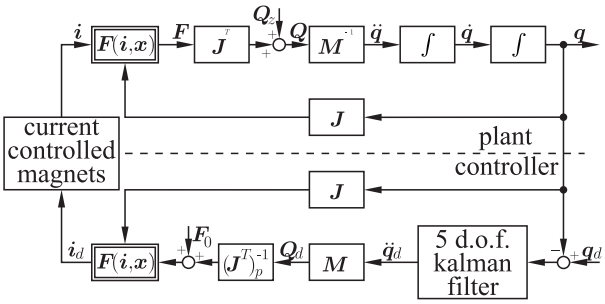

FIGURE 5: Control loop layout

the mass matrix $\boldsymbol{M}$ and the Jacobian $\boldsymbol{J} = \frac{\partial \boldsymbol{x}}{\partial \boldsymbol{q}}$, where the magnet displacements from the nominal air gap are given by the (8x1) vector $\boldsymbol{x} = \boldsymbol{s}_0 - \boldsymbol{s}$ and the guide displacement in generalized coordinates by the (5x1) vector $\boldsymbol{q}$.
The controller itself is designed in a normalized domain for a reference coordinate system, calculating the desired acceleration $\ddot{\boldsymbol{q}}_d$ from the the displacement $\Delta \boldsymbol{q}$ in a reference point. For an optimal suppression of sensor noise it is realized as 5 independent discrete-time optimal controllers with KALMAN filters for the observation of the guide velocities.
As the forces of the magnets can only be tensile, an offset of half the nominal maximum force is added. The current necessary to achieve the desired force is calculated using an inverse model of the magnet characteristics. Usually a linear relation

$$F = k_i i + k_s s \tag{1}$$

with gain k_i and negative bearing stiffness k_s is used, which in inverse formulation denotes

$$i = \frac{F - k_s s}{k_i}. \tag{2}$$

This linear formulation is well suited for differential magnet arrangements, where the nonlinearities of the magnets compensate each other. The control of the prototype guide relied on this linear model. In the proposed new single magnet arrangement the use of a linear model would lead to a controller fixed to one operating point. To make the control law applicable to a larger working range, a nonlinear formulation has to be introduced. The tensile forces of the direct drives can be easily included in this formulation. They are transformed via a Jacobian to forces and moments in the reference point [3].

NONLINEAR FORCE CHARACTERISTICS

As it is well known, the force of an electromagnet like in figure 6 results as

$$F = \frac{A}{2\mu_0} B^2 \tag{3}$$

with total pole area A, free space magnetic permeability μ_0 and flux density B. B itself depends on the magnetic field intensity H_0 in the air gap according to

$$B = \mu_0 H_0. \tag{4}$$

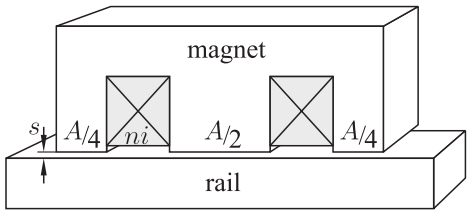

FIGURE 6: Sketch of an electromagnet

As long as saturation effects can be neglected, H_0 depends on the exciting magnetomotive force with current i and coil turns n as

$$2sH_0 = ni. \tag{5}$$

With eq. (3) the force depends on the square of the current and the inverse square of the air gap:

$$F = \frac{\mu_0 A}{8} \left(\frac{ni}{s}\right)^2. \tag{6}$$

With increasing flux density, the field intensity H_{Fe} in the iron is no longer negligible. H_{Fe} itself depends nonlinearly on B as

$$B = \mu_0 H_0 = \mu_{Fe}(B)\, H_{Fe}. \tag{7}$$

Figure 7 shows a typical saturation curve of the iron. Then, eq. (5) has to be expanded to

$$2sH_0 + \ell_{Fe} H_{Fe} = ni \tag{8}$$

with mean iron length ℓ_{Fe}. The distribution of the magnetomotive force of the exciting current to air gap and iron is shown in figure 8. It can be seen that up to about 1.2T saturation effects are negligible, whereas with higher flux densities the magnetomotive force in the iron becomes more dominating. According to these effects, eq. (6) has to be corrected. Eq. (8) yields

$$H_0 = \frac{ni - \ell_{Fe} H_{Fe}}{2s} \tag{9}$$

with H_{Fe}=$H_{Fe}(i,s)$. Thus, the force can be expressed as

$$F = \frac{\mu_0 A}{8} \left(\frac{ni - \ell_{Fe} H_{Fe}(i,s)}{s}\right)^2. \tag{10}$$

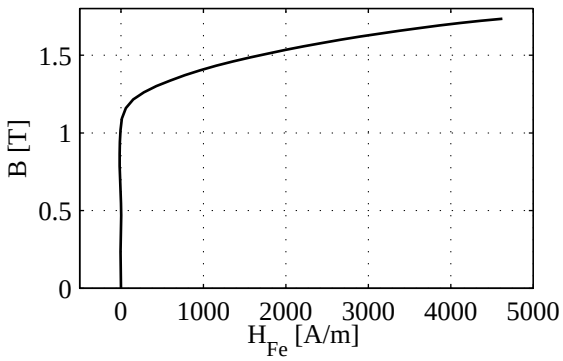

FIGURE 7: Saturation curve of the core iron (calculated from measurements, hysteresis neglected)

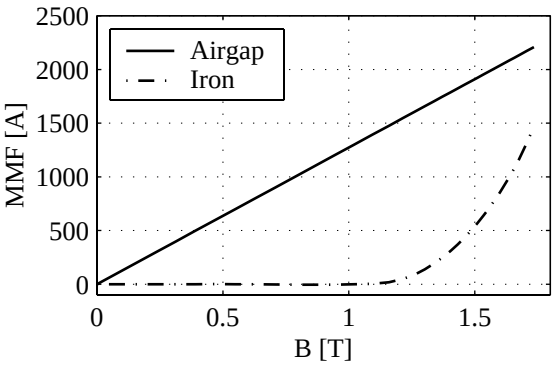

FIGURE 8: Distribution of the magnetomotive force to iron and air gap (s=0.8mm)

For the levitation control of the machine axis, it is necessary to know this relationship as accurately as possible. Although $H_{Fe}(i,s)$ can be calculated in advance if the permeability $\mu_{Fe}(B)$ of the iron is known, a better approach is to measure the force directly. For this purpose, a test rig (cp. figure 9) has been built. Furthermore, it is designed as a differential arrangement to examine the behaviour under control. The magnets are sourced by switched power amplifiers with a maximum current slope of $\frac{di}{dt}$=75kA/s at n=100 and a bandwidth of more than 5kHz. The force characteristics (cp. figure 10) show the proportionality to $(i/s)^2$ for forces below $4kN$ (about 1.2T at A=72cm^2) and the influence of the saturation for higher forces.

NONLINEAR COMPENSATION CONTROLLER

For the levitation control the inverse relationship of eq. (10) is required to calculate the desired current from the desired force at the present air gap of the magnet. Thus, eq. (10) yields

$$ni = \sqrt{\frac{8}{\mu_0 A}} s\sqrt{F} + \ell_{Fe} H_{Fe}. \qquad (11)$$

Theoretically, H_{Fe} can now be expressed as a function of F, as F depends only on B (cp. eq. (3)). Practically, with high flux densities the stray flux - which has been neglected so far - increases and reduces the available force. Measurements show the stray flux to increase approximately linear to the air gap. This requires an additional influence on H_{Fe}:

$$H_{Fe} = H_{Fe}(F,s). \qquad (12)$$

An approach to approximate the magnet force via analytical functions is given in [6]. There, 10 parameters are used to build this function. For real-time applications, especially of multi-degree-of-freedom systems as a magnetic guide, a simpler approximation is desired to reduce computational overhead. A polynomial approach of fourth order

$$\ell_{Fe} H_{Fe} = s \sum_{i=1}^{4} (a_i F^i) \qquad (13)$$

shows to be sufficient. This presents a moderate numerical effort compared to the multi-DOF control itself. The final equation for the nonlinear compensator denotes

$$ni = c_1 s(\sqrt{F} + c_2 F + c_3 F^2 + c_4 F^3 + c_5 F^4). \qquad (14)$$

It depends on 5 independent parameters $c_1 \ldots c_5$ which can be fitted to the measured force characteristics.
Figure 11 shows the characteristic surface of the compensator fitted to figure 10 and figure 12 the resulting linearization. The linearization can be seen to be successful over the whole working range (s=0.2..0.8mm, F=0..5000N) only with small deviations at small air gaps. This nonlinear compensator has been used successfully for the control of the test rig.

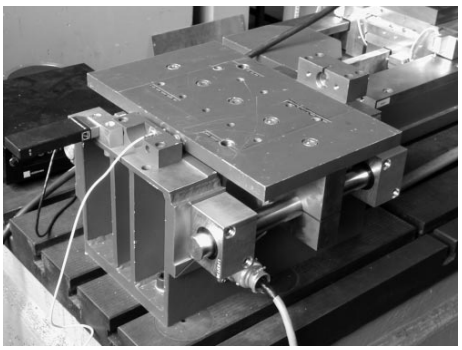

FIGURE 9: Test rig for examination of the magnet characteristics

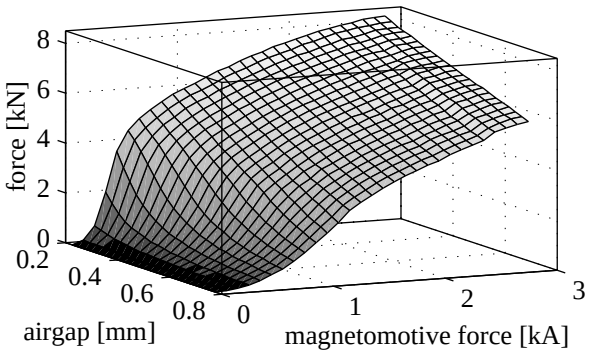

FIGURE 10: Measured magnet characteristics

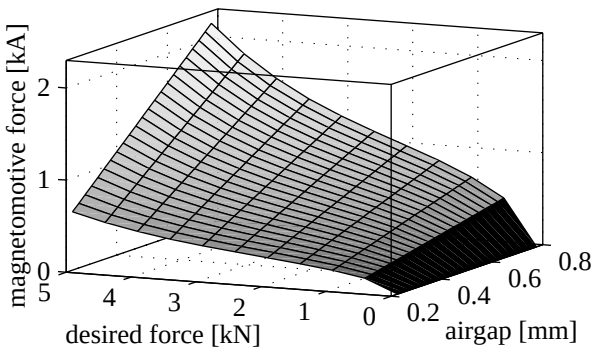

FIGURE 11: Identified nonlinear compensator

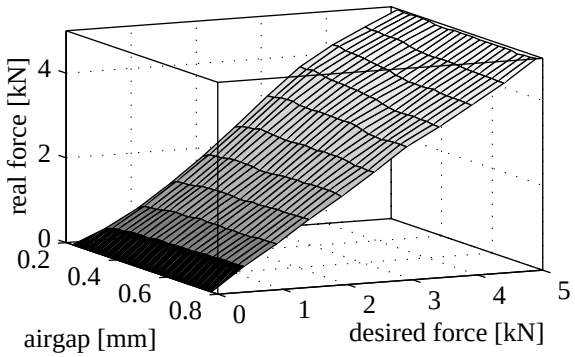

FIGURE 12: Linearized magnet characteristics

EDDY CURRENT EFFECTS

For the magnetic guides known so far, solid iron has been used for the rails. This was mainly for mechanical reasons, as for differential magnets it is very difficult to construct laminated rails with an adequate mechanical stiffness. Solid, non-laminated rails have one main disadvantage: eddy currents in the rails limit the dynamics of the flux density. Figure 13 shows the time signal of the flux density in a magnet of the test rig with a solid rail made of St37. The air gap has been fixed to 0.8mm. It can be clearly seen that for low frequencies almost only the hysteresis of the material is measured. For higher frequencies, however, induced eddy currents produce a noticeable decrease in amplitude and increase in phase shift.

With small scale electromagnets, these eddy current losses seem to be of relatively small influence. Figure 14 shows the Bode plot of the flux density per current for a magnet of the first prototype guide shown in figure 2 (A=10cm^2). For the main working range of the controller (0..300Hz) the amplitude loss is about 30% and the phase shift about 30°. These effects can be compensated using a first or second order discrete time filter. The amplitude loss reduces the available maximum dynamic force, but can be accepted in most applications. It must be assured that the power amplifiers can source the necessary current slope. Of course, a trade off is necessary between compensation success and noise sensitivity.

With the larger magnets for the test rig and the machine

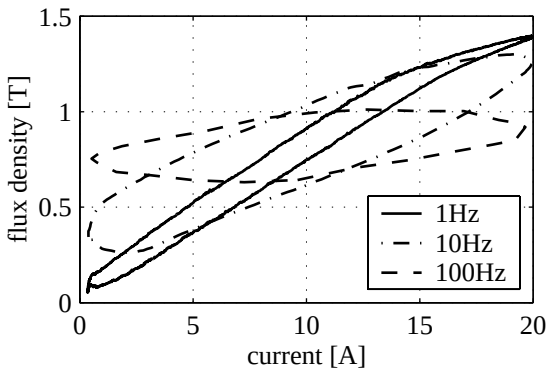

FIGURE 13: Time signal of the flux density on the test rig (St37-rail)

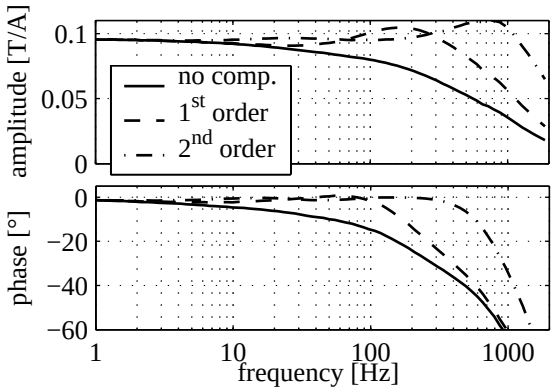

FIGURE 14: Bode plot of flux density for the first prototype guide with different compensation filters

axis, eddy current effects are more dramatic. Figure 15 shows the loss in amplitude and phase for solid and laminated rails, respectively. Obviously with massive rails the amplitude loss is about 75% at 150Hz and the phase shift about 60°. The measurements were taken at the center of the magnet poles. At the border the losses are smaller.

Although it is possible to compensate these effects with a filter as well, the loss in dynamic force amplitude is immense so that an application of solid rails to a large scale machine axis is limited to applications, where large force amplitudes are expected only at low frequencies (<10Hz) or high frequencies (>300Hz), where the inertial mass of the guide dominates the dynamic stiffness. Here, the force amplitude is sufficiently high. For the stability of the control a compensation filter according to figure 14 can be used. The effectiveness of this approach has been demonstrated on the test rig.

It could be expected that the eddy current effects impose a nonlinearity to the magnet dynamics. A nonlinearity analysis has been performed (cp. figure 16) showing that the nonlinearities represented by the upper harmonics of the flux density are negligible. Thus, the implementation of a linear eddy current compensation filter is allowable.

RESULTS

The final proof of a control strategy's effectiveness for a

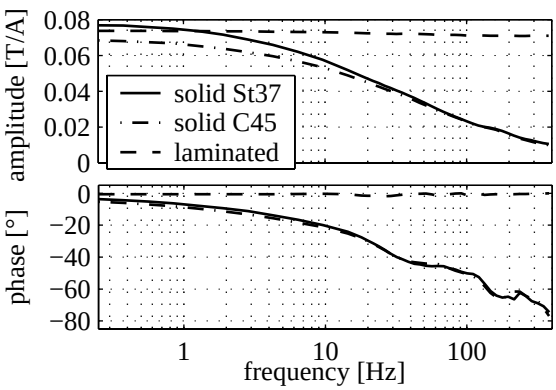

FIGURE 15: Bode plot of flux density for the test rig with different rail materials

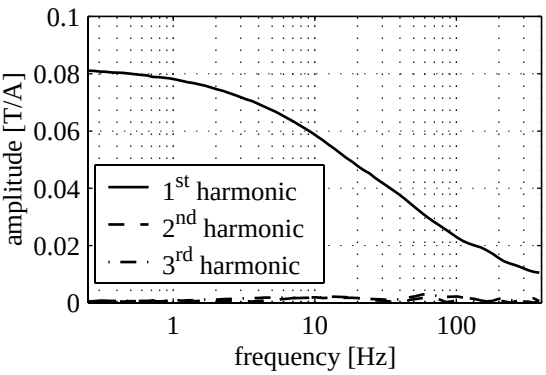

FIGURE 16: Harmonics of the flux density (St37)

magnetic guide is the measured compliance to an external force. Therefore, a force exciter has been fixed to the test rig. The excitation level was 50N. The measurements were taken with a solid St37 rail, as a laminated rail is not yet available for mechanical reasons. Two different eddy current compensation filters were used. Filter 1 has a maximum phase lift of about 15°, whereas filter 2 raises the phase by about 30°. Without a filter a stiff control was hardly possible.

Figure 17 shows that the more effective filter 2 limited the available maximum controller dynamics compared to filter 1. Nonetheless the resonance caused by the eddy current losses can be pushed to about 200Hz and reduced in amplitude so that the best stiffness is obtained. The maximum compliance of the control is 0.2μm/N. Therefore, the minimum stiffness in the whole frequency range is 5N/μm. The damping of the main resonance is nearly D=1, whereas a side resonance due to eddy current losses is less damped. With the use of laminated rails this resonance can be removed, making the controller even twice as stiff (cp. the flat maximum of the broken lines in figure 17).

As the controller is designed in a normalized domain, its achieved stiffness has to be related to the disturbance *acceleration*, as the mass (matrix) scales the stiffness outside the controller. The moving mass of the test rig is about 20kg. As the mass of the machine axis will be about 600kg, a theoretical minimal stiffness of 150N/μm

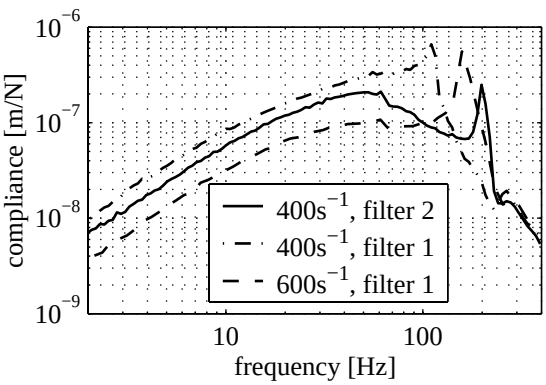

FIGURE 17: Compliance plots for different controllers and eddy current compensation filters

in the whole frequency range could be expected. This is significantly higher than the maximum value known so far of 35N/μm [3].

SUMMARY AND OUTLOOK

For new high speed machines magnetic guides qualify as an alternative to conventional roller guides. It has been shown in prototype experiments that the dynamic behaviour of a magnetic guides are satisfying. Even first milling tests have been performed. On a test rig the scaleability of the design has been proofed. A new single magnet arrangement has been proposed using a simple nonlinear model of the electromagnets. The model has been tested successfully on the test rig. Further, eddy current losses with solid rails have been discussed, whose effects can be reduced by compensating filters, though laminated rails show to be a better approach. The newly proposed machine axis design allows an easy implementation of laminated rails. Presently, a new high speed cutting machine is under construction which will be equipped with a magnetically guided axis. The first results make the expectation of a minimum dynamic stiffness of 150N/μm at a damping ratio near D=1 realistic. This stiffness makes the guides no longer the weakest part of the machine compared to the remaining mechanical structure.

REFERENCES

1. Tieste, K.-D., Mehrgrößenregelung und Parameteridentifikation einer Linearmagnetführung, PhD Thesis, VDI-Fortschrittsberichte Reihe 8, Band 656, Düsseldorf 1997.
2. Ruskowski, M. and Popp, K., A Contactless Machine Axis for High Speed Cutting Machines, Proc. 4th Int. Conference on Motion and Vibration Control MOVIC, Vol. 3, Zürich 1998, pp. 1095-1099.
3. Ben-Yahia, K. and Henneberger, G., Linear Magnetic Bearing For High Speed Machine Tool, Proc. Intelligent Motion, Nürnberg 1999, pp. 155-160.
4. Ruskowski, M., Popp, K., Tönshoff, H. K., Lapp, Ch. and Kaak, R., Auslegung einer Werkzeugmaschine mit kontaktloser Achse, 4. Magdeburger Maschinenbautage, Magdeburg 1999, pp. 105-112.
5. Tönshoff, H. K, Ahlers, H., Kaak, R. and Schubert, M., Design of a Hover-axis for a High-dynamic Machine Tool, Int. ADAMS Users' Conference, 17.-19. Nov., Berlin 1999 (on CD).
6. Hoffmann, K.-J. and Markert, R., Linearisierung von magnetischen Lagerungen für elastische Rotoren per Software, VDI-Berichte Nr. 1315, Düsseldorf 1997, pp. 407-418.
7. Ruskowski, M., Popp, K., Tönshoff, H. K. and Kaak, R., Modal Control of a Magnetically Guided Machine Axis, 20th International Congress of Theoretical and Applied Mechanics, Chicago 2000.